LRO-LAMP OBSERVATIONS OF LUNAR EXOSPHERIC HELIUM. C. Grava[1], D. M. Hurley[2], K. D. Retherford[1], G. R. Gladstone[1], T. K. Greathouse[1], K. E. Mandt[2]. [1]Southwest Research Institute, 6220 Culebra Road, San Antonio, TX, 78238, USA (cgrava@swri.edu), [2]Johns Hopkins University, Applied Physics Laboratory, Laurel, MD, USA.

Introduction: We present more than 150 observations of the lunar exospheric helium from the Lyman-Alpha Mapping Project (LAMP) ultraviolet spectrograph [1] on board the Lunar Reconnaissance Orbiter (LRO) [2] between 2013 and 2016. The emission line of HeI at 58.4 nm, due to resonant scattering of solar photons, is bright enough for the sensitive LAMP detector to observe during a single orbit, allowing for studies of temporal, latitudinal, and local time variations of the helium density.

Lunar exospheric helium, observed for the first time by the LACE spectrograph deployed on the lunar surface during the Apollo 17 mission [3], has its main origin in the neutralization, upon impact, of incident solar wind alpha particles [4]. Helium interacts weakly with the lunar regolith, therefore its density n is inversely proportional to the surface temperature T: $n \sim T^{-5/2}$ [5], and thus depends on the local time. However, a small but non-negligible fraction (between ~15% [6] and ~40% [7]) of the lunar helium outgasses from the interior of the Moon, as the radioactive daughter of ^{232}Th and ^{238}U [8]. Previous LAMP observations detected enhancements in the lunar He density uncorrelated with either local time or solar alpha particle flux [9], which seem to be the result of outgassing.

Observations: LAMP can detect the feeble emission lines of the tenuous lunar exosphere by pointing at the nightside, thus considerably suppressing the background, when the spacecraft is illuminated, and sunlit gases along the line of sight (LOS) resonantly scatter solar photons. By tilting LRO along its direction of motion (pitch maneuvers, like in Figure 1) and sideways (roll maneuvers), it is possible to considerably increase the illuminated LOS compared to the nominal, nadir mode, and hence to increase the brightness of the HeI emission line. By repeating these maneuvers over multiple orbits, it is possible to study the dependence of lunar helium density on local time, selenographic longitude, and solar wind conditions (as measured by the ARTEMIS twin spacecraft [10]). Each of these parameters is informative about a specific physical parameter:

- The dependence of the helium density with local time, and hence on lunar surface temperature, yields the degree of accommodation (and thus the interaction) between helium and the lunar surface temperature.
- The dependence of the helium density with selenographic longitude yields information on the possible locations of helium outgassing.
- The dependence of helium density on the solar wind alpha particle flux constrains the source rate and the amount of lunar endogenic helium (compared to the population from the solar wind).

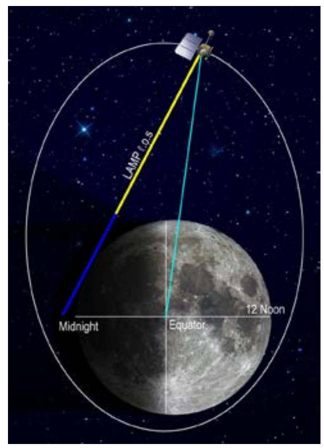

Figure 1 LAMP mode of observations during dedicated pitch campaigns (not to scale). The Moon view is centered on the sub-Earth point around last quarter. LRO is tilted along the direction of motion, and LAMP is observing the exosphere through the illuminated line of sight (yellow) towards the lunar nighttime surface. The blue line of sight is the portion of the lunar exosphere in shadow.

LAMP count rates are converted first to brightness by applying the instrument calibration factor obtained by looking at interstellar helium [11], and then to column density using daily averages of solar irradiance at 58.4 nm measured by the Solar Dynamic Observatory's Extreme ultraviolet Variability Experiment [12].

Data-model comparison: Line of sight column densities are compared with a Monte Carlo code of the lunar exosphere [13], which predicts the density of helium as a function of latitude, solar time, and altitude. The model is scaled to the solar wind alpha particles flux measured by ARTEMIS to account for the variability in the solar wind alpha particles flux (and hence of the helium source rate). For each point along the LAMP LOS we compute the column density predicted by the model.

As an example of data-model comparison, Figure 2 shows a scatter plot that compares LAMP-derived column densities (in the ordinates) vs model-predicted column densities, for two different accommodation factors.

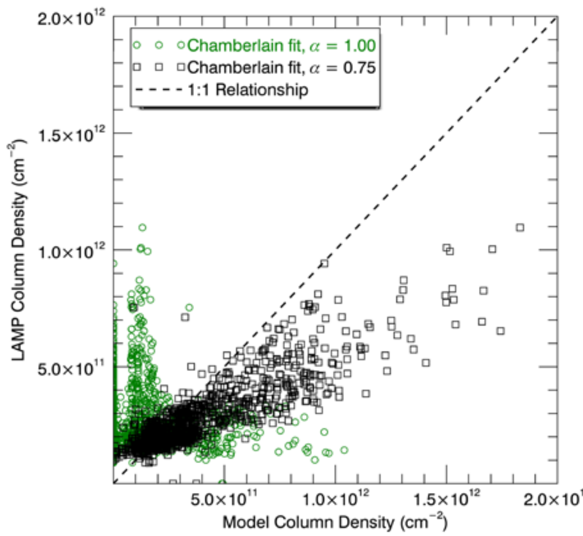

Figure 2 Data-model comparison: LAMP-derived column densities are plotted against model-predicted column densities. Black squares: model with accommodation coefficient (α) of 0.75. Green circles: model with α = 1.00. The dashed line indicates a 1:1 relationship, where a perfect model would align.

The accommodation factor α is a measure of the interaction between the exospheric atoms and the surface and is defined as $(E_{out}-E_{in})/(E_T-E_{in})$, where E_T is the mean energy per atom in thermal equilibrium with the surface, E_{in} is the mean energy per atom of the incoming particle, and E_{out} is the mean energy per atom of the particle that leaves the surface [14,15]. An accommodation coefficient of 1.00 means that the mean energy of the particle leaving the surface is equal to the mean energy of the particle in thermal equilibrium with the surface. In this case, therefore, the species bouncing off the surface "lose the memory" of their energy prior to the impact: the energy of the atoms leaving the surface will depend solely on the temperature of the regolith. LAMP observations show that the lunar exospheric helium is not fully thermalized and suggest that helium's accommodation coefficient lies between 1.00 and 0.75. Future models will further constrain this value.

References: [1] Gladstone G. R. et al. (2010) *Sp. Sci. Rev., 150(1-4)*, 161-181. [2] Chin G. et al. (2007) *Sp. Sci Rev., 129(4)*, 391-419. [3] Hoffman, J. H. et al. (1973), *LPSC IV*, 2865. [4] Hodges R. R. and Hoffman J. H. (1974) *GRL*, *1(2)*, 69-71. [5] Hodges R. R. and Johnson F. S. (1968), *JGR*, *73(23)*, 7307-7317. [6] Benna M. et al. (2015), *GRL*, *42*, *10*, 3723 - 3729; [7] Grava et al. (2016), *Icarus*, *273*, 36-44. [8] Hodges R. R. (1977), *LPSC VIII*, 537-549. [9] Cook J. C. & Stern S. A. (2014), *Icarus*, *236*, 48-55. [10] Angelopoulos, V. (2011), *Sp. Sci. Rev.*, *165*, 3–25. [11] Grava C. et al. (2018), *A&A*, 616, A159. [12] Woods T. N. et al. (2012), *Sol. Phys.*, *275*, 1-2, 115-143. [13] Hurley D. M. et al. (2016), *Icarus*, *273*, 45-52. [14] Leblanc F. and Chaufray, J.-Y. (2011), *Icarus*, *216*(2), 551-559. [15] Shemansky D. E. and Broadfoot A. L. (1977) *Rev. of Geophys.*, *15*(4), 491-499.